Plasma Phys. Control. Fusion 37 (1995) A279–A290. Printed in the UK

Linear and nonlinear evolution of alpha-particle driven gap modes

S. Briguglio, C. Kar, F. Romanelli, G. Vlad and F. Zonca
Associazione EURATOM-ENEA sulla Fusione,
C.R.E. Frascati, C.P. 65 00044, Frascati, Roma, Italy

Abstract. A discussion of linear dynamics and nonlinear evolution of modes belonging to the shear Alfvén branch is presented. Attention is focused to the modes which exist near the gap of the continuous spectrum. A discussion of the relative importance of mode-mode coupling, $E \times B$ trapping and stochastic losses is also presented.

I Introduction

Discrete modes can exist,[1] called toroidal Alfvén eigenmodes (TAE), in the gap of the continuous shear Alfvén spectrum, produced by the poloidal variation of the equilibrium associated to the effect of toroidicity.[2] They can be destabilized by the resonant interaction with the α particles since the Alfvén frequency is of the order of the α-particle transit frequency,[3] for typical parameters of an ignited plasma.

The TAE stability is a result of the competition among several effects. The transit resonance with the bulk-ions plays a strongly stabilizing role in the plasma core[4] and trapped electron collisional effects[5] may be important in the outer part of the discharge. Meanwhile, the α-particle drive is localized around the region of the maximum α-density gradient. Thus, the mode stability strongly depends on the radial mode localization which can be determined only by solving the fully 2-D eigenvalue problem.[6–8] Furthermore, for realistic parameters, the effect of the drive and damping terms cannot be treated perturbatively and should be considered at the same order at which toroidicity is important. A nonperturbative, fully 2-D analysis of the gap mode stability has been presented in Ref. [9] using a recently proposed theory of toroidal Alfvén modes. In the present paper, we will discuss the behaviour of the Alfvén spectrum for different toroidal mode numbers and ITER-like equilibria. A preliminary investigation of this problem, using perturbation theory in the drive and damping terms, has been presented in Ref. [11].

Early investigations of TAE-induced losses,[12] have shown that losses can be significant at very low mode amplitude. Since the mode is radially localized, the particle drift is large only close to the gap region, unless the threshold for orbit stochasticity is exceeded. In order to understand whether the nonlinear evolution of TAE finally results in mode saturation, stochastic losses or bursts similar to fishbones, the problem of nonlinear TAE evolution has received increasing attention. The nonlinear evolution can be dominated by mode-mode coupling[13,14] or by the energetic particles nonlinearities.[15] In the former case, saturation is due to the occurrence of a "singular" perturbation to the nonlinear mode structure which dissipates energy on very short

0741-3335/95/11A279+12$19.50

scale. In the latter case, saturation is due to the reduction in the mode drive, because a number of resonant particles become trapped in the wave and, on average, do not exchange energy with the mode. In this paper, a discussion of the relative importance of the two different nonlinear saturation mechanisms for TAE modes is given.

The plan of the paper is the following. In Section II the linear gap-mode stability is discussed. In Section III the problem of nonlinear saturation due to mode-mode coupling is analyzed. The saturation mechanism associated to the energetic particle nonlinearity is presented in Section IV. Section V is devoted to the problem of stochastic losses. Concluding remarks are given in Sec. VI.

II Linear gap mode stability

Since the most unstable modes correspond to moderately high toroidal mode numbers n, a stability analysis can be properly addressed in the context of the ballooning mode formalism. The global mode structure can then be modeled as a superposition of identical poloidal harmonics, characterized by a scale length of the order of the separation $1/nq'$ between neighboring rational surfaces, and modulated by a global envelope $A(r)$, varying on the equilibrium scales. Since the "fast" scale length which characterizes each harmonics and the "slow" scale length of the envelope are well separated, the eigenvalue problem can be solved in two steps on the basis of asymptotic theory: first, the structure of each harmonic is determined; second, the global envelope function is found. The structure of each harmonic is obtained by solving the 1-D local eigenvalue problem along the field lines. This leads to a "local" dispersion relation $F(\omega, r, \theta_k) = 0$, with θ_k being the radial wave vector associated with the slow envelope variation. The function $A(r)$ is determined at the next order in two-scale asymptotic expansion, by considering the radial variation of the equilibrium profiles. It has been shown[6–8] that the radial eigenmode problem, solved with WKB techniques, leads to the following equation for the global eigenvalue

$$\epsilon_T\, n \left[\int_{r_1}^{r_2} q'(r)\theta_k(r)dr + \theta_k(r_1)q(r_1) - \theta_k(r_2)q(r_2) \right] = (l+p)\pi \quad . \tag{1}$$

Here, $\theta_k(r)$ is implicitly defined by the local dispersion relation $F(\omega, r, \theta_k) = 0$ and $r_{1,2}$ are the (complex) WKB turning points, defined by the condition $\partial F/\partial\theta_k = 0$. By symmetry considerations, it can be shown that the turning points correspond to $\theta_k = \theta_k^{(T)}$, with $\theta_k^{(T)} = 0$ or $\theta_k^{(T)} = \pi$ because of the poloidal periodicity of the plasma equilibrium. Furthermore, in Eq.(1) l is the radial mode number, $\epsilon_T = 1$ if $\theta_k(r_1) = 0$ and $\epsilon_T = -1$ if $\theta_k(r_1) = \pi$ and $p = 1/2$ if the two turning points correspond to the same $\theta_k^{(T)}$ whereas $p = 0$ if they correspond to different $\theta_k^{(T)}$ values.

Thus, in the present approach, all the complexity of the description is contained in the derivation of the function $F(\omega, r, \theta_k)$. The local dispersion function F is obtained by solving the MHD equations, with the contribution of the energetic particles entering in the pressure tensor and being determined from the solution of the drift kinetic equation.[3] Since a complete discussion of the derivation of the local dispersion relation is outside the scope of this review, we will simply list the assumptions made in the analysis presented in Ref. [9,10].

The most important approximation is the use of an asymptotic expansion in the local inverse aspect ratio ϵ. Due to the existence of a smallness parameter ϵ, the "fast" radial variation (on the scale $1/nq'$) of a generic poloidal harmonic, in which the mode is decomposed, is further sub-divided into two-scale-length structures: a typical scale of the order a/n far from the gap location, with a being the minor radius, and a scale $\epsilon a/n$ in the gap region, where toroidal coupling is effective and causes a forbidden frequency gap to exist in the local shear Alfvén continuum. Even though the large aspect ratio expansion is a poor approximation for realistic equilibria, the qualitative behaviour of the Alfvén spectrum is correctly reproduced.

Finite-beta corrections are fully accounted for. These terms are very important since they may shift the mode frequency into the lower shear Alfvén continuum, as shown in Ref. [7]. For realistic ITER parameters, the Alfvén spectrum corresponds indeed to modes which are almost entirely located in the continuum. In order to determine the bulk-plasma beta effect, a model circular equilibrium with shifted flux surfaces (the conventional (s, α) model) is employed.

Modes located in the continuum are singular in the ideal MHD limit. To remove the singularity, non ideal effects such as finite thermal-ion Larmor-radius (FLR) corrections must be retained. Since these terms are important only near the singular points, their effect can be retained only in the gap region. They modify the continuous shear-Alfvén spectrum into a spectrum of discrete modes (KTAE) with a typical frequency separation of the order $\delta\omega^{KTAE}/\epsilon\omega_A \approx k_\theta \rho_i s/\epsilon^{3/2}$, with k_θ being the poloidal wavevector, ρ_i the ion Larmor radius and ω_A the Alfvén frequency. The associated eigenfunctions are radially localized, with a typical mode width of the order $\epsilon a k_\theta \rho_i/\epsilon^{3/2}$ ($\approx 0.1a$ for ITER parameters and $n \approx 10$), as shown in Ref. [10]. Thus, in addition to the TAE branch, also its kinetic counterpart (the KTAE[16]) is described by Eq.(1).

In the present analysis, drive and damping terms are treated non-perturbatively. This allows to investigate the stability of a branch of forced plasma oscillations which would not exist in the absence of energetic particles: the energetic-particle continuum modes (EPM).[10,17] The EPM excitation is similar to the $n = 1$ fishbone mode.[18] Its frequency is related to the transit frequency of the energetic particles, rather than to the Alfvén frequency characteristic of the MHD modes. As shown in Ref. [10], the EPM is the analytic continuation of the KTAE at large values of the α-particle drive. These modes are characterized by a growth rate larger than $\delta\omega^{KTAE}$. Thus, in this respect, their behaviour is described by the ideal MHD equations, and they see the discrete KTAE spectrum as an ideal continuum.

Energetic-particle finite-orbit corrections are accounted for by considering two different limits. If the orbit width is comparable with or smaller than the gap width ($k_\theta \rho_h << \epsilon$, with ρ_h the energetic-particle Larmor radius), the energetic particle contribution is located in the gap region. For shorter wavelengths, instead, the energetic particle contribution mainly comes from the region outside the gap. Thus, the linear growth-rate may be expected to linearly increase with n until the condition $k_\theta \rho_h \approx \epsilon$ is satisfied. For larger toroidal mode numbers, the growth-rate is independent of n and, for $k_\theta \rho_h \gtrsim 1$, the growth-rate decreases as n^{-3}, as shown in Ref. [10,17].

Equation (1) is difficult to handle analytically in order to derive mode frequency and radial envelope function. Thus, for a full two-dimensional global stability analysis which uses Eq. (1), a numerical code has been developed,[9] which determines the "Stokes structure" of the complex r-plane associated to the local dispersion function, and then finds global frequency spectra.

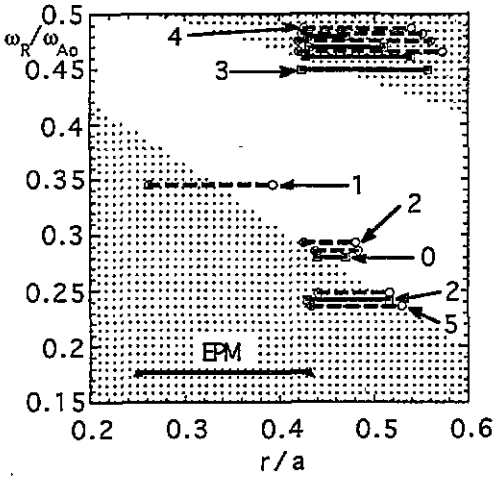

Figure 1. Radial location of the turning points and real frequency. The considered toroidal mode numbers are $n = 10$ (solid lines) and $n = 20$ (dashed lines). The dotted area is the Alfvén continuum. Few radial mode numbers l are indicated. Also an unstable EPM (with $n = 10$ and $l = 0$) corresponding to a drive with $\hat{\beta}_E = 2$ is shown.

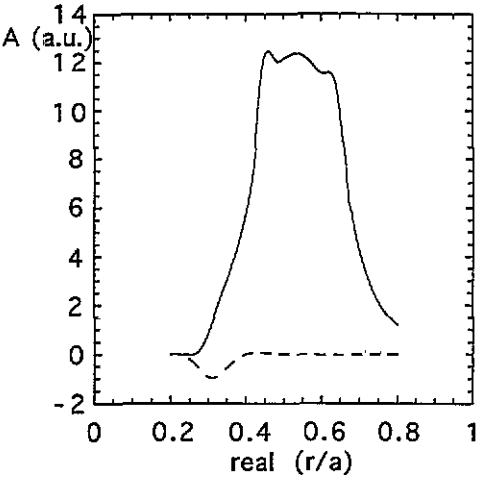

Figure 2. Real (solid curve) and imaginary (dashed curve) part of the envelope $A(r)$ of the various poloidal harmonics corresponding to a TAE eigenfunction with $n = 10$ and $l = 0$ is shown. Here the bulk plasma has $\beta = 0$ and the real frequency, normalized to the Alfvén frequency in the center, is $\omega_R/\omega_{A0} = 0.385$.

In the following we will consider applications to ITER-like parameters. The α-particle density n_α is evaluated from the condition $n_\alpha =< \sigma v > n_{DT}^2/4\tau_{sd}$, $n_{DT} = n_e/2$, with $\tau_{sd}(s) = 1.2 \times 10^{-2} T_e(keV)^{3/2}/n_e(10^{20}m^{-3})$. The equilibrium profiles are given by $n_e = n_o(1 - r^2/a^2)^{\alpha_n}$, $T = T_o(1 - r^2/a^2)^{\alpha_T}$, yielding $p_\alpha = p_{\alpha_o}(1 - r^2/a^2)^{\alpha_h}$, with $\alpha_h = \alpha_n + 3.5\alpha_T$, $T_o = 20keV$, $n_o = 1.5 \times 10^{20}m^{-3}$, $\alpha_n = 0.5$ and $\alpha_T = 1$.

The Alfvén spectrum is shown in Fig.1 for a case in which drive and Landau damping terms have been neglected. The dotted regions indicate the Alfvén continuum. The thick lines connect the projections onto the real axis of the (complex) turning points, thus showing the radial localization of the modes. The considered toroidal mode numbers are $n = 10$ and $n = 20$. A dense spectrum of KTAE and mixed TAE/KTAE modes, corresponding to different radial mode numbers l, are shown. These modes suffer a considerable damping, in the absence of an α-particle drive, because of finite ion Larmor radius effects. In Fig.1 also an unstable EPM is shown

(with $n = 10$ and $l = 0$) with a drive corresponding to $\hat{\beta}_E = \beta_E/\beta_{\alpha,0} = 2$, where β_E is the energetic-(α)-particle beta and $\beta_{\alpha,0} \approx 0.015$ corresponds to the central α-particle beta of the reference ITER scenario (note that because of the strong dependence of β_E on the bulk-plasma temperature, a 20% increase in the bulk plasma temperature is sufficient to rise β_E by a factor 2).

The envelope $A(r)$ of the various poloidal harmonics corresponding to a TAE eigenfunction is shown in Fig.2. In this case, $n = 10$, $l = 0$ and $\beta = 0$ has been assumed for the bulk-plasma. As the bulk-plasma β increases, the mode, whose real frequency for $\beta = 0$ lies inside the Alfvén continuum gap, is shifted toward the lower continuum, becoming a mixed TAE/KTAE mode, as the ones shown if Fig.1. These modes are more localized along the minor radius than a pure TAE.

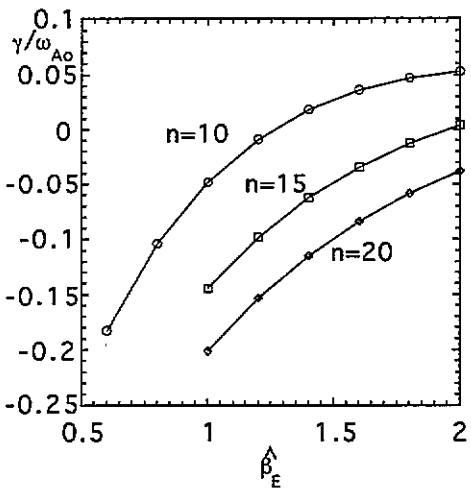

Figure 3. Growth-rate γ, normalized to the Alfvén frequency in the center ω_{A0}, for EPM with $l = 0$ and $n = 10, 15, 20$ vs. the energetic particle drive $\hat{\beta}_E$.

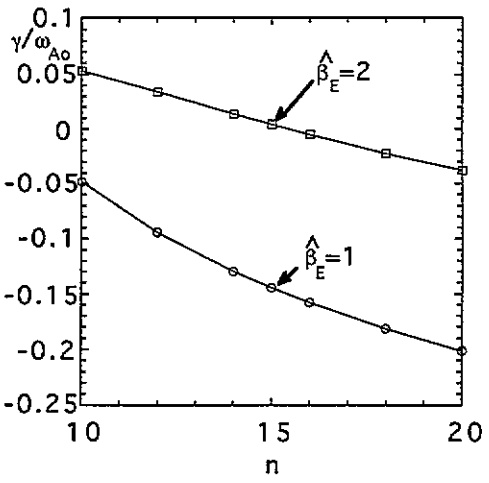

Figure 4. Growth-rate γ, normalized to the Alfvén frequency in the center ω_{A0}, for EPM with $l = 0$ vs. n. Two different values of the energetic particle drive $\hat{\beta}_E$ are considered.

The stability of an EPM mode as $\hat{\beta}_E$ increases is shown in Fig.3. The considered modes have $l = 0$ and $n = 10, 15, 20$. The real frequency of the modes is strongly modified as β_E increases, shifting the real frequency of the mode from the gap to the lower continuum. The threshold for instability is close to $\hat{\beta}_E = 1.25$ for $n = 10$ and increases with increasing toroidal mode number (see Fig.4).

From the above considerations the following scenario emerges. On ITER, pure TAE modes will be absent in a large portion of the discharge due to finite-β effects, although, close to the magnetic axis where $s^2 < \epsilon$ it has been recently shown that core localized TAE modes may exist.[19] Thus, only radially localized KTAE will be present. However, at large α-particle beta (e.g. 20% larger than the reference ITER value for $n = 10$), the relevant instability is the EPM.

III Nonlinear saturation due to mode-mode coupling

The problem of nonlinear saturation due to mode-mode coupling has been investigated in Ref. [14], where it has been shown that mode saturation is due to nonlinear ion Compton scattering, and in Ref. [13]. In the latter case, the plasma dynamics is assumed to be described by the reduced $O(\epsilon^3)$ MHD equations with the perpendicular velocity $\mathbf{v}_\perp \equiv (R^2/R_o)\nabla U \times \nabla\zeta$ and the magnetic field $\mathbf{B} \equiv R_o\nabla\Psi \times \nabla\zeta + R_o B_o \nabla\zeta$. Let us consider two harmonics (m,n) and $(m+1,n)$ of a TAE eigenfunction, interacting at the gap location $r = r_o$ where $q(r_o) = (2m+1)/2n$. It has been shown in Ref. [13] that the dynamics of the two harmonics in the gap region is described, in the high-n limit, by the following system

$$\begin{aligned}\left(\hat{\omega} - \hat{\omega}_o - i\Gamma_\alpha - 4i\mu\partial_x^2 - 2sx\right)\partial_x u + \partial_x v - C_u - 4\partial_x u\,|\partial_x v|^2 = 0 \\ \left(\hat{\omega} - \hat{\omega}_o - i\Gamma_\alpha - 4i\mu\partial_x^2 + 2sx\right)\partial_x v + \partial_x u - C_v - 4\partial_x v\,|\partial_x u|^2 = 0\ . \end{aligned} \qquad (2)$$

Here, $\hat{\omega} \equiv 2\omega/(\epsilon_o\omega_o)$, $\hat{\omega}_o = 2/\epsilon_o$, $\mu = m^2\eta/(\omega_o r_o^2 \epsilon_o^3)$, η is the plasma resistivity, $s = r_o q_o'/q_o$ is the magnetic shear, $\epsilon_o = 2\Delta' + r_o/R_o$, with Δ' being the derivative of the Shafranov shift, ω_o is the Alfvén frequency at the gap center and $x \equiv 2m(r-r_o)/(r_o\epsilon_o)$. Furthermore, $u(x)$ and $v(x)$ are the (m,n) and $(m+1,n)$ Fourier components of the stream function U normalized to $U_o^{-1} \equiv (2/\epsilon_o)^{3/2}(m^2/\omega_o r_o^2)$ and the two quantities C_u and C_v are obtained from the dissipationless linear cylindrical equations outside the gap region and are, at the lowest order, proportional to the mode amplitude A. The system Eqs.(2) together with the boundary conditions $u, v \to 0$ as $|x| \to \infty$, defines an eigenvalue problem, with the eigenvalue being the (nonlinear) frequency ω. The condition $Im[\omega(A)] = 0$ defines the saturation value of the mode amplitude A.

Let us consider first the linear limit by neglecting the cubic nonlinearities in Eqs.(2). If the TAE mode is not close to the gap boundary, its dynamics is weakly affected, by the presence of dissipation during the linear phase. Thus, the mode will grow in time at a rate determined by the α-particle drive, which, in the above equation, is modelled by a constant term Γ_α. Note that, in linear theory, the shear Alfvén continuum is determined by the vanishing of the Jacobian of the Eqs.(2), yielding, in the absence of α-particle drive,

$$\hat{\omega} - \hat{\omega}_o = \pm\left[1 + 4s^2x^2\right]^{1/2}\ , \qquad (3)$$

with the continuum accumulation points at $\hat{\omega} - \hat{\omega}_o = \pm 1$.

The nonlinear interaction of the (m,n) and $(m+1,n)$ harmonics produces $(1,0)$ and $(2m+1,2n)$ beat components which can be explicitly evaluated and originate the cubic nonlinear terms in Eqs.(2). Let us assume that dissipation continues to be negligible also in the nonlinear phase. Equations (2), then, are a system of nonlinear algebraic equations in the two unknowns $\partial_x u$ and $\partial_x v$ which can be solved as long as the Jacobian J of the system continues to be different from zero over the entire x domain, with J given by

$$J = \left[\delta\omega - 2sx - 4(\partial_x v)^2\right]\left[\delta\omega + 2sx - 4(\partial_x u)^2\right] - \left[1 - 8\partial_x u\partial_x v\right]^2\ , \qquad (4)$$

where $\delta\hat{\omega} \equiv \hat{\omega} - \hat{\omega}_o - i\Gamma_\alpha$ is a real quantity.

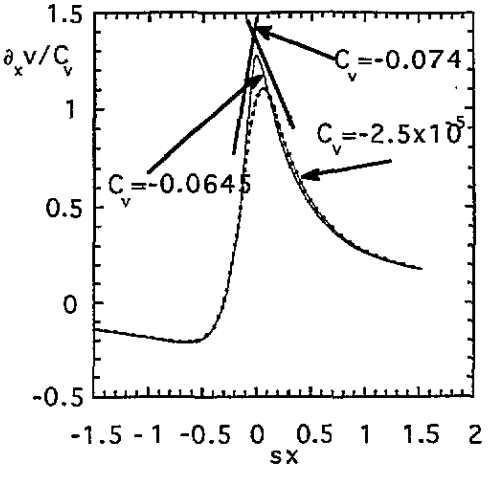

Figure 5. Nonlinear eigenfunction for various amplitude. Saturation occurs at $C_v = -0.074$.

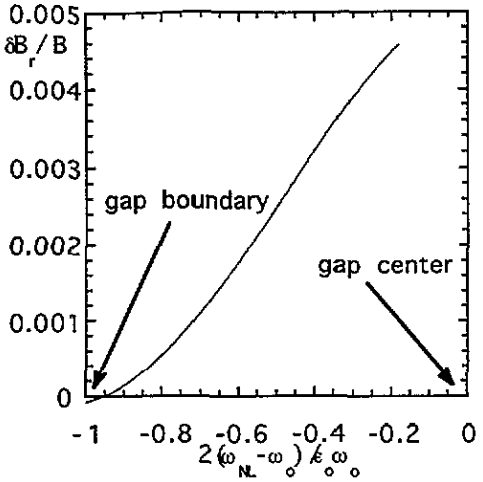

Figure 6. Saturation amplitude vs. nonlinear eigenfrequency.

However, as the amplitude increases, the nonlinear modification to J becomes important and, as a critical threshold for the mode amplitude is approached, the Jacobian tends to vanish and the mode structure tends to develop a singularity in the form of a cusp point,[13] as shown in Fig.5. In such a situation, the assumption of small resistive dissipation effects, which has been made above, becomes invalid. The local mode structure will change, since very small scales get excited nonlinearly. The damping due to resistive dissipation is then expected to rapidly increase above the linear estimate, and nonlinear mode saturation occurs when the mode drive is balanced by the nonlinear damping. This picture for the TAE saturation has been verified using a numerical code which solves the nonlinear reduced MHD equations.

For the case $n = 1$, $m = 1,2$ and a model equilibrium $q = q(0) + (q(a) - q(0))(r/a)^2$, $q(0) = 1.1$ and $q(a) = 1.9$, it is possible to show that saturation occurs for $|\delta B_{r1,1}(r_o)/B_o| \simeq 2.21 \times 10^{-2}(a/R_o)^{5/2}$. Thus, a simple estimate for the mode saturation amplitude is

$$\left|\frac{\delta B_r(r_o)}{B_o}\right| \simeq \frac{c_o}{m}\left(\frac{a}{R_o}\right)^{5/2} , \tag{5}$$

with c_o being a function of the distance of the nonlinear mode frequency from the gap boundary and, for the considered q-profile, of the order $c_o \approx 2.21 \times 10^{-2}$.

It is clear, from this simple picture of the saturation due to mode-mode coupling, that such a mechanism is more important for eigenmodes with a narrow structure already in the linear phase, i.e. with a frequency close to the Alfvén continuum.

This is shown in Fig.6, where the saturated amplitude of the $m = 1$ harmonic of a $n = 1$ a TAE eigenfunction is shown as a function of the nonlinear mode frequency. As the frequency approaches the gap boundary, the mode structure in the gap region becomes narrower and a lower amplitude is required in order to excite the short scales which produce dissipation. Thus, we can expect such a mechanism to be important, in principle, also for KTAE modes which are located in the Alfvén continuum. The nonlinear saturation of EPM is still to be explored, even though we may expect to be similar to the nonlinear saturation of fishbones.

IV Energetic particles nonlinearity

The resonant energetic particles are those satisfying $|\omega - k_{\|}(r)v_{\|}| \lesssim \gamma_L$, where γ_L is the linear mode drive. The particles in resonance with the wave are thus contained within a distance Δr_R from the flux surface r_o, where the mode is localized:

$$\frac{\Delta r_R}{r_o} \simeq \frac{\gamma_L}{\omega}\frac{1}{ms} \ . \tag{6}$$

The number of resonant particles trapped in the TAE wave can be obtained from the particles equation of motion $v_r = \dot{r} = v_{\|}(\delta B_r/B) + c\delta\mathbf{E}\times\mathbf{b}\cdot\nabla r/B$, yielding

$$\dot{r} = \frac{c}{\omega B}\nabla\delta\phi\times\mathbf{b}\cdot\nabla r\left(k_{\|}v_{\|}-\omega\right) \ .$$

Now, the resonance condition for energetic particles is $\omega = k_{\|}v_{\|} + \mathbf{k}_{\perp}\cdot\mathbf{v}_D$, where $\mathbf{v}_D = -v_{Do}(\sin\theta\nabla r + r\cos\theta\nabla\theta)$ is the particles magnetic drift, $v_{Do} = (v_{\perp}^2/2 + v_{\|}^2)/R\omega_c$, ω_c is the cyclotron frequency and (r,θ,ζ) is a right-handed toroidal coordinate system, with ζ being the toroidal angle. From the above equation it is possible to show that trapped particles oscillate within a distance Δr_T such that

$$\frac{\Delta r_T^2}{r_o^2} \lesssim \frac{v_{Do}}{v_{\|}}\frac{qR}{s\omega}\frac{1}{r_o^2}\frac{c}{B}\frac{\partial\delta\phi_o}{\partial r}$$

from the surface r_o.[15] Since particles which are trapped in the wave do not exchange, on average, energy with the mode, we may expect that nonlinear saturation occurs if $\Delta r_T \gtrsim \Delta r_R$. Thus, the amplitude at which significant trapping occurs can be roughly estimated as

$$\frac{\delta B_r}{B} \approx \frac{\epsilon_o^2}{s^2q^2m^2}\frac{r_o}{\rho_h}\left(\frac{\gamma_L}{\omega}\right)^2 \ . \tag{7}$$

In order to understand the relative importance of this mechanism with respect to mode-mode coupling, let us assume as a typical saturation level for the TAE mode the value given in Eq.(5), obtained in the previous section and valid for a mode frequency not too close to the gap boundary. The condition for neglecting energetic particles nonlinearities reads

$$\left(\frac{\gamma_L}{\omega}\right)^2 \gtrsim c_o\left(\frac{\rho_h}{r_o}\right)m\epsilon_o^{1/2}q^2s^2 \ .$$

Here, ρ_h is the energetic particles Larmor radius. Taking $r_o/\rho_h \approx 30$ and $\epsilon_o \approx (1/3)$ as typical values, the condition on the linear mode drive to neglect energetic particles nonlinearities is $\gamma_L/\omega \gtrsim 3 \times 10^{-2}$ for $m = 1$. This result suggest that the stronger the linear drive, the more relevant the effect of fluid nonlinearities may be.[13]

In order to check the validity of these arguments we have performed particle simulations of the nonlinear saturation of the mode. A gyrokinetic code[20] is used to compute the nonlinear response of an energetic-particle population to a TAE-like electromagnetic perturbation. We consider fluctuating potentials of the form $f_{m,n}(\mathbf{r},t) = A(t)\exp(-i\omega t)\, f_{0_{m,n}}(\mathbf{r})$, where $\omega = \omega_r - i\gamma_d$, ω_r is the (fixed) real frequency of the perturbation, γ_d is a small damping (representative of the several damping mechanisms not considered in detail in these simulations) and the amplitude $A(t)$ is evolved in time according to

$$\frac{dA}{dt} = \gamma_{NL} A \quad . \tag{8}$$

Here, γ_{NL} takes into account the energetic-particle nonlinear response and is computed at each time step in terms of the energetic-particle contribution to the potential energy δW_K and of the plasma kinetic energy K_M, as[4]

$$\gamma_{NL} \simeq \frac{v_A}{R_0}\, Im \lim_{Im\omega \to 0} \delta W_K / K_M \simeq -\frac{1}{2\rho_h}\frac{v_h}{R_0}\frac{m_h}{m_i}\frac{n_{h0}}{n_0}\, Re\, \frac{\int d^3r\, \delta\hat{p}\, \hat{\mathbf{b}} \times \nabla R \cdot \nabla \hat{\phi}^*}{\int d^3r\, |\nabla_\perp \hat{\phi}|^2}, \tag{9}$$

where $\delta\hat{p}$ is the (normalized) energetic-particle perturbed pressure, $\hat{\phi}$ the (normalized) scalar fluctuating potential, and v_h, m_h, and n_{h0} are respectively the thermal velocity, the mass and the on-axis density of the energetic particles. Moreover, v_A is the Alfvén velocity, whereas m_i and n_0 are the bulk-ion mass and density respectively.

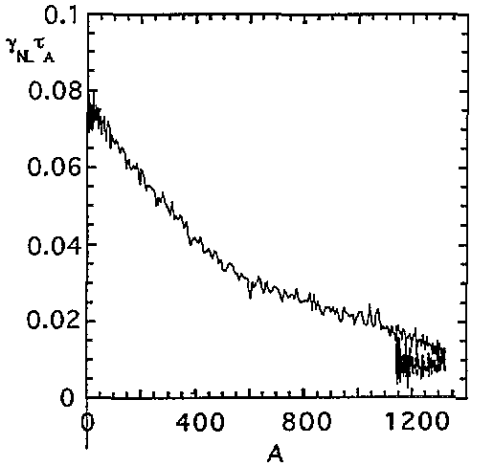

Figure 7. Nonlinear drive, normalized to $\tau_A \equiv R/v_A$, as a function of the amplitude of the mode for a typical particle simulation.

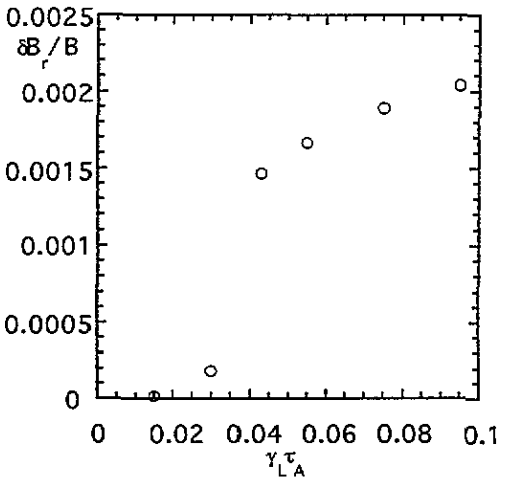

Figure 8. Saturation amplitude, of the $m = 1, n = 1$ harmonic, vs. linear growth rate.

Note that the influence of the energetic particles on the spatial structure of the perturbation as well as on its real frequency is neglected. Similar simulations of the TAE nonlinear dynamics have been made in Ref. [21].

The saturation level strongly depends on the (unknown) dependence of γ_{NL} on the amplitude A. Figure 7 shows such dependence, as resulting from a simulation with a spatial grid of $N_r \times N_\theta \times N_\varphi = 64 \times 16 \times 8$ cells and an average number of 64 particles per cell, and the following choice of the parameters: $a/R_0 = 0.1$, $v_h/v_A = 1$, $n_{h0}/n_0 = 0.02$, $m_h/m_i = 2$, $\rho_h/a = 0.01$, $\omega_* = -(1/3)v_A/R_0$, $\gamma_d = 0.01 v_A/R_0$. An energetic-particle density profile $n_h(r) = n_{h0} \exp\left[-(r^2/L_n^2)^{\alpha_n}\right]$, with $\alpha_n = 2$ and $a^2/L_n^2 = 2$, has been assumed. The amplitude at saturation is shown in Fig.8 vs γ_L. Note that at large γ_L a departure from the quadratic behaviour is observed.

V Stochastic losses

So far, the problem of the relative importance of energetic particles nonlinearities vs. mode-mode coupling effects has been considered. The hence derived result indicates generally comparable saturation levels for both mechanisms, the latter being more important for strong linear drive. In general, it is possible to embrace both results assuming that the mode saturates when the trapped (in the TAE wave) particles deviation from the reference flux surface $\Delta r_T/r_o$, as given by Eq. (6), satisfies the condition

$$\frac{\Delta r_T}{r_o} \simeq \frac{\gamma_L}{\omega} \frac{1}{Kms} , \tag{10}$$

K being a numerical factor. Clearly, for $K \approx 1$ the saturation is likely due to particles nonlinearities, while, for $K >> 1$ the saturation mechanism is due to mode-mode coupling. Equation (10) is a criterion for the mode saturation based on the island width of the perturbed particle orbits and independent of the specific saturation mechanism.

Equation (10) may be used to derive a condition for the transition to stochastic particle orbits, independent of the considered saturation mechanism. Assume that the radial cross section of the torus, of minor radius a, is filled by TAE turbulence with assigned spectrum in poloidal and toroidal mode numbers (m, n). Each (m, n) harmonic generates a small island of width $\delta r_{m,n}$ in the particle trajectory. The transition to stochastic orbits is expected to occur when

$$\sum_{m,n} \delta r_{m,n} \gtrsim a .$$

From Eq. (10), it is possible to estimate $\delta r_{m,n} \approx (\gamma_L/\omega)(a/Kms)$. Thus, the above condition for stochasticity becomes

$$\sum_{m,n} \frac{\gamma_L}{\omega} \frac{1}{Kms} \gtrsim 1 . \tag{11}$$

The summation in (m, n) can be carried out explicitly noting that, for each toroidal mode number n, approximately $nq(r_o)\epsilon_o$ poloidal harmonics are excited around the

central mode number $m_o = nq(r_o)$ in the high-n limit.[6,7] Furthermore, the energetic particle drive γ_h, as a function of the mode number, is conveniently modeled as $\gamma_h \simeq (n/n_1)\gamma_o$ ($\gamma_o \simeq \beta_h\omega$), for $n < n_1$ ($n_1 = \epsilon_o a/q(r_o)\rho_h$); $\gamma_h \simeq \gamma_o$, for $n_1 < n < n_2$ ($n_2 = a/q(r_o)\rho_h$); and $\gamma_h \simeq \gamma_o(n_2/n)^2$, for $n > n_2$.[17] The net drive $\gamma_L = \gamma_h - \gamma_d$ is obtained assuming a constant background dissipation γ_d, independent of the mode number. In the m summation, the net drive may be assumed constant. Therefore, performing the summation in Eq. (11) for $\gamma_L > 0$, one obtains

$$\sum_n \frac{\epsilon_o}{K}\frac{\gamma_L}{\omega} = \frac{\epsilon_o}{K}\frac{\gamma_o}{\omega} n_2 \left[1 - \frac{n_1}{n_2} + \frac{n_1^2 - n_\ell^2}{2n_1 n_2} + \frac{1}{2}\left(1 - \frac{n_2^2}{n_\ell^2}\right) - \frac{\gamma_d}{\gamma_o}\left(\frac{n_u}{n_2} - \frac{n_\ell}{n_2}\right)\right] \gtrsim 1 \ . \quad (12)$$

Here, $n_\ell \equiv n_1(\gamma_d/\gamma_o)$ and $n_u \equiv n_2(\gamma_o/\gamma_d)^{1/3}$ are the lower and upper cut-offs in the mode number summation, at which $\gamma_L = 0$. Equation (12) gives a threshold in the linear mode drive for the transition to stochastic particle orbits, which is independent of the particular considered saturation mechanism. The threshold in the linear mode drive is equivalent to a threshold in the energetic particles β_h, which typically reads

$$\frac{\gamma_o}{\omega} \simeq \beta_h \gtrsim \frac{K}{\epsilon_o n_2} \simeq \frac{Kq R_o \rho_h}{a^2} \ .$$

This condition may be difficult to be satisfied, except for particularly low values of K. Taking e.g. ITER parameters, $\beta_h \approx 5.4 \times 10^{-3}$ and $R_o\rho_h/a^2 \approx 1.5 \times 10^{-2}$.Thus, stochastic losses are unlikely to occur.

The above estimate for the onset of stochastic losses should be compared with the estimate for a single toroidal harmonic n given in Ref. [22] $\beta_h \gtrsim 1/[20q^{5/2}n^{1/2}]$. Stochastic losses have been observed in Ref. [12] for $\delta B_r/B \approx 10^{-3}$ in a simulation where a $n = 1$ linear eigenfunction was taken, with m ranging between $m = 1$ and $m = 3$. Further developments are needed in order to draw definitive conclusions.

VI Conclusions

In the present paper a review of the linear and nonlinear dynamics of modes belonging to the shear Alfvén branch has ben presented. On the basis of linear theory and taking the parameters of a reference ITER scenario, TAE is stable or close to marginal stability over a large portion of the discharge (with the possible exception of the low shear region where core localized TAE modes can exist[19]). Finite beta effects are crucial in causing the mode to strongly interact with the lower continuum. The radial eigenmode analysis predicts very localized KTAE eigenfunctions. The most important instability should be the energetic particle mode.

Saturation mechanisms associated to mode-mode coupling may be particularly important if the radial mode width is narrow, as in the case of modes close to the gap boundary or inside the continuum. Saturation due to phase space trapping leads to values for the saturated amplitude comparable to those obtained in the case of mode-mode coupling. The saturated amplitude increases with the linear growth-rate. Thus, we expect that mode-mode coupling will be more effective for the most unstable

modes. An estimate for the onset of stochastic losses has been also given. For typical ITER parameters this kind of loss mechanism is unlikely to occur.

References

[1] C.Z. Cheng, Liu Chen, and M.S. Chance, Ann. Phys. **161**, 21, (1985).

[2] C.E. Kieras, and J.A. Tataronis, J. Plasma Phys. **28**, 395, (1982).

[3] Liu Chen, *Theory of Fusion Plasmas* (Editrice Compositori Societa' Italiana di Fisica, Bologna,1988), p. 327.

[4] R. Betti, J.P. Freidberg, Phys.Fluids B4, 1465, (1992)

[5] V.A. Mazur, A.B. Mikhailovskij, Nucl. Fusion **17**, 193 (1977); N.N. Gorelenkov, S.E. Sharapov Phys. Scr. **45**, 163, (1992)

[6] F. Zonca and Liu Chen, Phys. Rev. Lett. **68**, 592, (1992).

[7] F. Zonca and Liu Chen, Phys. Fluids B **5**, 3668, (1993).

[8] F. Zonca, Ph.D. Thesis, Princeton University, Plasma Physics Laboratory, Princeton N.J. (1993).

[9] G. Vlad, F. Zonca and F. Romanelli submitted to Nucl. Fusion

[10] F. Zonca and Liu Chen submitted to Phys. Plasmas

[11] F. Romanelli and F. Zonca, *Tokamak Concept Improvement* (Editrice Compositori Societa' Italiana di Fisica, Bologna,1994), p. 191.

[12] D.J. Sigmar, C.T. Hsu, R. White, C.Z. Cheng, Phys. Fluids B **4**, 1506 (1992)

[13] F. Zonca, F. Romanelli, G. Vlad, and C. Kar, Phys. Rev. Lett. **74**, 698 (1995); G. Vlad, C. Kar, F. Zonca, and F. Romanelli, Phys. of Plasmas **2**, 227 (1995).

[14] T.S. Hahm and Liu Chen Phys. Rev. Lett. **74**, 266 (1995).

[15] H.L. Berk, and B.N. Breizman, Phys. Fluids B **2**, 2246, (1990).

[16] R.R. Mett and S.M. Mahajan, Phys. Fluids B **4**, 2885 (1992); G.Y. Fu and C.Z. Cheng, Phys. Fluids B **4**, 3722 (1992); J.W. Connor et al. *21st EPS Conference on Contr. Fus. and Pl. Phys.*, vol. II p.614 (1994)

[17] S.T. Tsai and Liu Chen, Phys. Fluids B **5**, 3284, (1993); Liu Chen, Phys. Plasmas **1**, 1519 (1994)

[18] L. Chen, R.B. White and M.N. Rosenbluth, Phys. Rev. Lett. **52**, 1122 (1984)

[19] G.Y. Fu, submitted to Phys. Plasmas; H.L. Berk et al., to appear in Phys. Plasmas

[20] S. Briguglio, G. Vlad, F. Zonca, and C. Kar, to be published on Phys. Plasmas.

[21] Y. Wu and R.B. White, Phys. Plasmas **1**, 2733 (1994)

[22] H.L. Berk, B.N. Breizman, H. Ye, Phys. Fluids B **5**, 1506 (1993)